AIMS Mathematics, 10(12): 29765–29783.
DOI: 10.3934/math.20251308
Received: 11 October 2025
Revised: 28 November 2025
Accepted: 08 December 2025
Published: 17 December 2025

https://www.aimspress.com/journal/Math

Research article

Soliton solutions of the time-fractional Poisson-Nernst-Planck system with stochastic analysis and their application

Waseem Razzaq[1], **Asim Zafar**[1], **Abdulaziz Khalid Alsharidi**[2] **and Mohammed Ahmed Alomair**[3,*]

[1] Department of Mathematics, COMSATS University Islamabad, Vehari Campus, Pakistan
[2] Department of Mathematics and Statistics, College of Science, King Faisal University, Al Ahsa 31982, Saudi Arabia
[3] Department of Quantitative Methods, School of Business, King Faisal University, Al-Ahsa 31982, Saudi Arabia

* **Correspondence:** Email: ma.alomair@kfu.edu.sa.

Abstract: This study investigated the influence of Brownian motion and noise effects on the dynamics of the stochastic Poisson-Nernst-Planck system with M-truncated fractional derivative. To explore exact analytical representations of the soliton solutions, the study employed the modified extended direct algebraic method. The method successfully produces closed-form exact soliton solutions that capture the stochastic behavior of the system in the presence of random perturbations. The addition of the M-truncated fractional derivative provides a more flexible structure to describe anomalous transport, offering an advanced mathematical representation of electro-diffusion processes. The obtained results highlight the combined role of noise, fractional dynamics, and stochastic fluctuations in shaping the system's evolution, thereby deepening the theoretical understanding of nonlinear stochastic transport models and opening potential avenues for applications in complex biological and physical systems. Moreover, the study presented graphical demonstrations that illustrate the effect of noise and the fractional order of derivation in 3D, 2D, and contour surfaces.

Keywords: Brownian motion; M-truncated fractional derivative; stochastic Poisson-Nernst-Planck system; modified extended direct algebraic method; exact soliton solution; noise effects
Mathematics Subject Classification: 35A20, 35C08, 35Q55, 37K10

1. Introduction

In applied sciences and mathematical physics, nonlinear evolution equations (NLSEEs) are crucial instruments. These equations explain the nonlinear changes in physical quantities like energy, particles,

waves, or charges over time and space. In contrast to linear equations, this complex phenomena, including soliton waves, shocks, dispersion, turbulence, and chaotic dynamics, can be modeled using NLEEs. Driven by this modeling, they are therefore frequently used in many different fields, such as quantum mechanics, fluid dynamics, optical communication, plasma, and biological transport systems.

Modeling the movement of charged particles, such as ions in a fluid or electrons in a semiconductor, is one of the main applications of NLEEs. Particle mobility in such systems is affected by electric fields in addition to concentration gradients. In recent decades, scientists and mathematicians have created numerous models in recent decades that describe detailed behaviors in systems including semiconductors, biological tissues, fluids, and plasmas. A list of such core models include the FitzHugh–Nagumo model [1], the Landau–Lifshitz model [2], the reaction-diffusion models [3], the (2 + 1)-dimensional KdV model [4], the Kuramoto-Sivashinsky model [5], the $(n+1)$-dimensional generalized Kadomtsev–Petviashvili model [6], the perturbed Gerdjikov-Ivanov model [7], and the generalized Korteweg-de Vries equations [8]. The classical Nernst-Planck equation was first proposed by Walther Nernst in 1888 to describe ion diffusion. Max Planck later included electric field effects, which resulted in the modern form of the Nernst-Planck equation currently in use. When it is coupled with the Poisson equation, the Poisson-Nernst-Planck (PNP) system is created, which connects the electric field and charge density. Furthermore, ion channels in biological membranes, semiconductor devices, electrochemical systems, and nanofluidic devices have all been described using this concept. They employ the Poisson-Nernst-Planck (PNP) system, a well-known nonlinear model, to mathematically characterize this linked behavior. This model consists of two components: the Poisson equation, which specifies how the charge distribution generates the electric potential, and the Nernst-Planck equations, which describe ion transport. A couple of nonlinear partial differential equations is the resultant PNP system. In domains such as biology, electrochemistry, and semiconductors, it is among the most potent models for explaining electro-diffusive transport.

As technology developed, scientists discovered that random fluctuations are frequently present in real-world systems because of internal interactions, external changes, or thermal noise. In order to account for these impacts, stochastic variations of the PNP system were created. These models are known as stochastic Poisson-Nernst-Planck (SPNP) systems [9] and they incorporated noise or random variables to allow for uncertainty. These are particularly helpful in biological systems, where random behaviors significantly affect system performance, such as neuron signaling and nanoelectronics.

To find exact soliton solutions of nonlinear systems like the PNP model, many analytical techniques have been developed. These include the Hirota Bilinear technique [10], the Lie symmetry method [11], Painlevé analysis [12], the tanh-coth method [13], the sine–cosine method [14], the extended sinh-Gordon equation expansion method [15], the $\frac{G'}{G}$-expansion approach [16], the exp-function method [17], the modified simple equation method [18], the Riccati equation mapping method [19], and the trial equation method [20].

While many PDEs have been successfully solved using these techniques, stochastic or highly nonlinear systems frequently present challenges. Noticing the concern, the present work focuses on finding soliton solutions that play a significant role in the field of applied sciences, where various applications exist [21, 22]. In order to enhance the soliton solution process, academics have suggested extended and modified algebraic approaches. The modified extended direct algebraic (MEDA) method is one such effective strategy. Additionally, the traditional direct algebraic method has been enhanced by this approach. Because of its adaptable solution structure, it can handle complex wave profiles,

such as solitary waves, periodic waves, and even solutions for rational functions. Its main advantages include the MEDA's simplicity, algebraic structure, and effective handling of both linear and nonlinear components.

Several researchers have applied the MEDA to different types of equations with success. For example, Waqar et al. [23] used the MEDA to find diverse wave solutions for the (2 + 1)-dimensional Zoomeron equation, Ashraf et al. [24] used the MEDA to find traveling wave solutions of the Hirota–Ramani equation, Qawaqneh et al. [25] discovered exact solitons to the fractional KP-MEW equation, and Amer et al. [26] used the MEDA to examine exact solutions to the Shynaray-IIA equation. Shahzad et al. [27] used the Meda to find the explicit solitary wave structures for the fractional-order Sobolev-type equations.

This study is aimed at establishing exact analytical soliton solutions of the 1D stochastic Poisson-Nernst-Planck system using the modified extended direct algebraic method. Using the MEDA method the study develops several exact solutions, such as soliton solutions, periodic wave profiles, and rational function solutions. This paper presents a novel analytical approach to stochastic PDEs and advances the mathematical description of ionic transport in noisy systems. The results demonstrate the effectiveness and simplicity of the MEDA method in solving complex nonlinear stochastic models. It might also be used as a guide for upcoming research in biology, engineering, and physics that uses different stochastic models.

• ***M*-truncated derivative**

Definition 1.1. The truncated Mittag–Leffler function is defined as follows:

$$ {}_i\mathbb{E}_\beta(g(z)) = \sum_{m=0}^{i} \frac{g(z)^m}{\Gamma(\beta m + 1)}, \tag{1.1} $$

where $g \in \mathbb{C}$ and $\beta > 0$.

Definition 1.2. Let $v : [0, \infty) \to R$ be a function. The M-truncated derivative of v of order α, where $\alpha \in (0, 1)$ with respect to z, is defined as

$$ \mathbb{D}_{(M,z)}^{(\alpha,\beta)} v(z) = \lim_{h \to 0} \frac{v(z + {}_i\mathbb{E}_\beta(hz^{-\beta})) - v(z)}{h}, \beta, z > 0, \tag{1.2} $$

where ${}_i\mathbb{E}_\beta(.)$ is the truncated Mittag-Leffler function.

• **Brownian motion**

Brownian motion shows the random walk of the particles in various fields where particles are in motion. It is defined as:

Definition 1.3. The stochastic procedure $\Re_t$, $t \geq 0$, holds for the following:

(1) $\Re_t = 0$,
(2) $\Re_t$ is continuous and has independent increments,
(3) $\Re_t$-$\Re_s$ has a Gaussian distribution,

it is called Brownian motion.

Lemma 1.1. $\mathbb{E}(e^{\delta \Re_t}) = e^{\frac{1}{2}\delta^2 t}$ for $\delta \in \mathbb{R}$, $\delta > 0$.

Key contributions of our work

- We formulate a stochastic PNP system that incorporates noise effects and M-truncated fractional derivatives to more accurately represent anomalous electro-diffusion and stochastic perturbations.

- We employ the modified extended direct algebraic method to derive new exact closed-form soliton solutions that capture the nonlinear stochastic dynamics of the system.
- We analyze the interplay between fractional dynamics, Brownian motion, and stochastic fluctuations, demonstrating their combined impact on the system's evolution.
- We provide a detailed graphical investigation, including 2D plots, 3D surfaces, and contour illustrations, to demonstrate the effects of noise intensity and fractional-order parameters on the solution profiles.

These additions clearly identify the research gap and outline the specific contributions of the present study.

This paper is organized as follows: Section 2 presents the wave transformation, Section 3 describes the scheme and its application, Section 4 discusses the fractional and noise effects on the graphs, and Section 5 concludes the study.

2. Governing model

In this section, we consider the steady state of a one-dimensional model of the PNP system, and we use the assumption that ion concentration would be constant across the channel section; it takes the following form:

$$\frac{\partial n_1}{\partial t} + \frac{\partial \mathbb{J}_1}{\partial t} = 0, \ with \ \mathbb{J}_1 = -g_1\left(\frac{\partial n_1}{\partial x} + \frac{z\mathbb{F}}{\mathbb{R}\mathbb{T}} n_1 \frac{\partial u}{\partial x}\right), \tag{2.1}$$

$$\frac{\partial n_1}{\partial t} + \frac{\partial \mathbb{J}_2}{\partial t} = 0, \ with \ \mathbb{J}_2 = -g_2\left(\frac{\partial n_1}{\partial x} + \frac{z\mathbb{F}}{\mathbb{R}\mathbb{T}} n_1 \frac{\partial u}{\partial x}\right), \tag{2.2}$$

and

$$\frac{\partial^2 u}{\partial x^2} = -\frac{z\mathbb{F}}{\epsilon_\alpha}(N_1 - N_2). \tag{2.3}$$

Given that the channel has a few angstroms of diameter and that the surrounding membrane is thought to be planar, the channel can be considered to be cylindrical. So, we assumed that N_1 and N_2 are fluxes and n_1 and n_2 are ionic concentrations that are assumed as constants. Here, $\mathbb{R}$ represents the universal gas constant, $\mathbb{T}$ is taken as the absolute temperature, $\mathbb{F} = eN_\alpha$ denotes Faraday's constant, Z denotes the charge's valence, u denotes the electric potential, x denotes the position membrane, and ϵ_α denotes the dielectric constant in the ionic solution. D is the diffusion coefficient of the ionic species. The electromigration is represented by the first term on the right side of the equation, while the solvent convection is shown by the second term. The above-mentioned fourth-order PNP system can be expressed in the simplest form as follows:

$$\mathbb{Q}\Psi_{xt} - \mathbb{Q}d\Psi_{xxx} - \mathbb{P}\mathbb{Q}\Psi_x\Psi_{xx} = 0. \tag{2.4}$$

Here, we assume that $\mathbb{P} = \frac{\epsilon_\alpha}{z\mathbb{F}}$, $\mathbb{Q} = \frac{\mathbb{F}z}{\mathbb{R}\mathbb{T}}$. The stochastic PNP system is considered in the following form:

$$\mathbb{Q}\Psi_{xt} - \mathbb{Q}d\Psi_{xxx} - \mathbb{P}\mathbb{Q}\Psi_x\Psi_{xx} - \mu B(t)\Psi_x = 0. \tag{2.5}$$

Now, we use the M-truncated fractional derivative definition for the time variable and get the time-fractional 1D stochastic Poisson-Nernst-Planck (TFSPNP) model such as:

$$\mathbb{Q}D_t^\alpha(D_x) - \mathbb{Q}dD_{xxx} - \mathbb{P}\mathbb{Q}D_xD_{xx} - \mu B(t)D_x = 0, \tag{2.6}$$

where α is between $0 < \alpha < 1$.

3. Wave transformation

To derive the wave equation for the stochastic PKP equation, we use the transformation

$$\Psi(x,t) = \Psi(\eta)e^{\mu B(t)-\frac{1}{2}(\mu)^2 t}, \quad \eta = vx + \frac{c\Gamma(\beta+1)}{\alpha}t^{\alpha}. \tag{3.1}$$

Here, $\Psi(\eta)$ is a real function, while c is the speed of the wave, and v is the amplitude of the wave.

We take the derivative of Eq (2.6), and we get

$$\Psi_x = v\Psi' e^{\mu B(t)-\frac{1}{2}(\mu)^2 t}, \Psi_{xx} = v^2\Psi'' e^{\mu B(t)-\frac{1}{2}(\mu)^2 t},$$

$$\Psi_{xxx} = v^2\Psi''' e^{\mu B(t)-\frac{1}{2}(\mu)^2 t}, \Psi_{xt} = [cv\Psi'' + \mu v\Psi' B(t)]e^{\mu B(t)-\frac{1}{2}(\mu)^2 t}.$$

By substituting these derivatives along with Eq (3.1) into Eq (2.6), we get

$$\Psi'' - \mathbb{Q}dv^3\Psi''' - \mathbb{P}d\Psi'\Psi'' e^{\mu B(t)-\frac{1}{2}(\mu)^2 t} = 0. \tag{3.2}$$

Now, by taking expectation $\mathbb{E}(.)$ [28], on both sides of Eq (3.2), we get:

$$\Psi'' - \mathbb{Q}dv^3\Psi''' - \mathbb{P}\Psi'\Psi''\mathbb{E}e^{(\mu B(t))}e^{-\frac{1}{2}(\mu)^2 t} = 0. \tag{3.3}$$

$B(t)$ is the time noise, and then $\mathbb{E}e^{(\mu B(t))} = e^{\frac{1}{2}(\mu)^2 t}$ in Eq (3.3) turns into:

$$\Psi'' - \mathbb{Q}dv^3\Psi''' - \mathbb{P}d\Psi'\Psi'' = 0. \tag{3.4}$$

Now, by integrating Eq (3.4), we have

$$\Psi' - \mathbb{Q}dv^3\Psi'' - \frac{\mathbb{P}d}{2}(\Psi')^2 = C. \tag{3.5}$$

Here we take the integrating constant zero.

$$\Psi' - \mathbb{Q}dv^3\Psi'' - \frac{\mathbb{P}d}{2}(\Psi')^2 = 0. \tag{3.6}$$

Let $\Psi' = \Re$, and Eq (3.6) takes the following form:

$$\mathbb{Q}dv^3\Re' + \frac{\mathbb{P}d}{2}(\Re)^2 - \Re = 0. \tag{3.7}$$

4. Modified extended direct algebraic method and its application

Some of the main steps are given as:

Step 1: Assuming a non-linear PDE:

$$H(\Re, \Re^2, \Re^2\Re_x, \Re_{xx}, \Re_{xt}, ...) = 0. \tag{4.1}$$

Here $\Re = \Re(x,t)$ denotes a wave function. We assume the following transformation:

$$\Re(x,t) = \mathfrak{Q}(\eta), \quad \eta = x + c\,t. \tag{4.2}$$

Putting Eq (4.2) into Eq (4.1) yields

$$G(\mathfrak{Q}, \mathfrak{Q}^2\mathfrak{Q}^{'}, \mathfrak{Q}^{''}, ...) = 0. \tag{4.3}$$

Step 2: Suppose the results of Eq (4.3) are shown as

$$\mathfrak{Q}(\eta) = \sum_{i=0}^{m} \mathfrak{w}_i \zeta^i(\eta). \tag{4.4}$$

Here $\mathfrak{w}_i (i = 0, 1, 2, 3, ..., m)$ are unknown. Function $\zeta(\eta)$ fulfills the given equation.

$$\zeta^{'}(\eta) = \log(\mathfrak{A})\left(r_1 + r_2\zeta(\eta) + r_3\zeta(\eta)^2\right). \tag{4.5}$$

Here r_1, r_2, and r_3 are constants and $\mathfrak{A} \neq 0, 1$. Consider the solutions of Eq (4.5) in the following cases: Case 1: when $\Omega = r_2^2 - 4r_1r_3 < 0$ and $r_3 \neq 0$:

$$\zeta(\eta) = -\frac{r_2}{2r_3} + \frac{\sqrt{-\Omega}\tan_P(\frac{1}{2}\sqrt{-\Omega}\eta)}{2r_3}, \tag{4.6}$$

$$\zeta(\eta) = -\frac{r_2}{2r_3} - \frac{\sqrt{-\Omega}\cot_P(\frac{1}{2}\sqrt{-\Omega}\eta)}{2r_3}, \tag{4.7}$$

$$\zeta(\eta) = -\frac{r_2}{2r_3} + \frac{\sqrt{-\Omega}(\tan_P(\sqrt{-\Omega}\eta) \pm (\sqrt{\omega\nu}\ \sec_P(\sqrt{-\Omega}\eta)))}{2r_3}, \tag{4.8}$$

$$\zeta(\eta) = -\frac{r_2}{2r_3} - \frac{\sqrt{-\Omega}(\cot_P(\sqrt{-\Omega}\eta) \pm (\sqrt{\omega\nu}\ \csc_P(\sqrt{-\Omega}\eta)))}{2r_3}, \tag{4.9}$$

$$\zeta(\eta) = -\frac{r_2}{2r_3} + \frac{\sqrt{-\Omega}(\tan_P(\frac{1}{4}\sqrt{-\Omega}\eta) - (\ \cot_P(\frac{1}{4}\sqrt{-\Omega}\eta)))}{2r_3}. \tag{4.10}$$

Case 2: when $\Omega = r_2^2 - 4r_1r_3 > 0$ and $r_3 \neq 0$:

$$\zeta(\eta) = -\frac{r_2}{2r_3} - \frac{\sqrt{\Omega}\tanh_P(\frac{1}{2}\sqrt{\Omega}\eta)}{2r_3}, \tag{4.11}$$

$$\zeta(\eta) = -\frac{r_2}{2r_3} - \frac{\sqrt{\Omega}\coth_P(\frac{1}{2}\sqrt{\Omega}\eta)}{2r_3}, \tag{4.12}$$

$$\zeta(\eta) = -\frac{r_2}{2r_3} - \frac{\sqrt{\Omega}(\tanh_P(\sqrt{\Omega}\eta) \pm (\sqrt{\omega\nu}\ sech_P(\sqrt{\Omega}\eta)))}{2r_3}, \tag{4.13}$$

$$\zeta(\eta) = -\frac{r_2}{2r_3} - \frac{\sqrt{\Omega}(\coth_P(\sqrt{\Omega}\eta) \pm (\sqrt{\omega\nu}\ csch_P(\sqrt{\Omega}\eta)))}{2r_3}, \tag{4.14}$$

$$\zeta(\eta) = -\frac{r_2}{2r_3} - \frac{\sqrt{\Omega}(\tanh_P(\frac{1}{4}\sqrt{\Omega}\eta) - (\ \coth_P(\frac{1}{4}\sqrt{\Omega}\eta)))}{2r_3}. \tag{4.15}$$

Case 3: when $r_1 r_3 > 0$ and $r_2 = 0$:

$$\zeta(\eta) = \sqrt{\frac{r_1}{r_3}} \tan_P(\sqrt{r_1 r_3}\eta), \tag{4.16}$$

$$\zeta(\eta) = -\sqrt{\frac{r_1}{r_3}} \cot_P(\sqrt{r_1 r_3}\eta), \tag{4.17}$$

$$\zeta(\eta) = \sqrt{\frac{r_1}{r_3}}(\tan_P(2\sqrt{r_1 r_3}\eta) \pm (\sqrt{\omega\nu}\sec_P(2\sqrt{r_1 r_3}\eta))), \tag{4.18}$$

$$\zeta(\eta) = -\sqrt{\frac{r_1}{r_3}}(\cot_P(2\sqrt{r_1 r_3}\eta) \pm (\sqrt{\omega\nu}\csc_P(2\sqrt{r_1 r_3}\eta))), \tag{4.19}$$

$$\zeta(\eta) = \frac{1}{2}\sqrt{\frac{r_1}{r_3}}(\tan_P(\frac{1}{2}\sqrt{r_1 r_3}\eta) - \cot_P(\frac{1}{2}\sqrt{r_1 r_3}\eta)). \tag{4.20}$$

Case 4: when $r_1 r_3 < 0$ and $r_2 = 0$:

$$\zeta(\eta) = -\sqrt{-\frac{r_1}{r_3}} \tanh_P(\sqrt{-r_1 r_3}\eta), \tag{4.21}$$

$$\zeta(\eta) = -\sqrt{-\frac{r_1}{r_3}} \coth_P(\sqrt{-r_1 r_3}\eta), \tag{4.22}$$

$$\zeta(\eta) = -\sqrt{-\frac{r_1}{r_3}}(\tanh_P(\sqrt{-r_1 r_3}2\eta) \pm (\iota\sqrt{\omega\nu}sech_P(\sqrt{-r_1 r_3}2\eta))), \tag{4.23}$$

$$\zeta(\eta) = -\sqrt{-\frac{r_1}{r_3}}(\coth_P(\sqrt{-r_1 r_3}2\eta) \pm (\sqrt{\omega\nu}csch_P(\sqrt{-r_1 r_3}2\eta))), \tag{4.24}$$

$$\zeta(\eta) = -\frac{1}{2}\sqrt{-\frac{r_1}{r_3}}(\tanh_P(\frac{1}{2}\sqrt{-r_1 r_3}\eta) + \coth_P(\frac{1}{2}\sqrt{-r_1 r_3}\eta)). \tag{4.25}$$

Case 5: when $r_3 = r_1$ and $r_2 = 0$:

$$\zeta(\eta) = \tan_P(r_1\eta), \tag{4.26}$$

$$\zeta(\eta) = -\cot_P(r_1\eta), \tag{4.27}$$

$$\zeta(\eta) = \tan_P(r_1 2\eta) \pm (\sqrt{\omega\nu}\sec_P(r_1 2\eta), \tag{4.28}$$

$$\zeta(\eta) = -\cot_P(r_1 2\eta) \pm (\sqrt{\omega\nu}\csc_P(r_1 2\eta), \tag{4.29}$$

$$\zeta(\eta) = \frac{1}{2}\tan_P(\frac{1}{2}r_1\eta) - \frac{1}{2}\cot_P(\frac{1}{2}r_1\eta). \tag{4.30}$$

Case 6: when $r_3 = -r_1$ and $r_2 = 0$:

$$\zeta(\eta) = -\tanh_P(r_1\eta), \tag{4.31}$$

$$\zeta(\eta) = -\coth_P(r_1\eta), \tag{4.32}$$

$$\zeta(\eta) = -\tanh_P(r_1 2\eta) \pm (\iota\sqrt{\omega\nu}sech_P(r_1 2\eta), \tag{4.33}$$

$$\zeta(\eta) = -\coth_P(r_1 2\eta) \pm (\sqrt{\omega\nu}csch_P(r_1 2\eta), \tag{4.34}$$

$$\zeta(\eta) = -\frac{1}{2}\tanh_P(\frac{1}{2}r_1\eta) - \frac{1}{2}\coth_P(\frac{1}{2}r_1\eta). \tag{4.35}$$

Case 7: when $r_2^2 - 4r_1r_3 = 0$:

$$\zeta(\eta) = -2\frac{r_1(r_2\eta\log(\mathfrak{A}) + 2)}{r_2^2\eta\log(\mathfrak{A})}. \tag{4.36}$$

Case 8: when $r_2 = \delta$, $r_1 = \delta m$ $(m \neq 0)$, and $r_3 = 0$:

$$\zeta(\eta) = \mathfrak{A}^{\delta\eta} - m. \tag{4.37}$$

Case 9: when r_2, $r_3 = 0$:

$$\zeta(\eta) = r_1\,\eta\log(\mathfrak{A}). \tag{4.38}$$

Case 10: when r_1, $r_2 = 0$:

$$\zeta(\eta) = -\frac{1}{r_3\,\eta\log(\mathfrak{A})}. \tag{4.39}$$

Case 11: when $r_1 = 0$ and r_2, $r_3 \neq 0$:

$$\zeta(\eta) = -\frac{\mu r_2}{r_3(\cosh_P(r_2\eta) - \sinh_P(r_2\eta) + \mu)}, \tag{4.40}$$

$$\zeta(\eta) = -\frac{r_2(\cosh_P(r_2\eta) + \sinh_P(r_2\eta))}{r_3(\cosh_P(r_2\eta) + \sinh_P(r_2\eta) + \nu)}. \tag{4.41}$$

Case 12: when $r_2 = \delta\ r_3 = m\delta$ $(m \neq 0)$, and $r_1 = 0$:

$$\zeta(\eta) = \frac{\mu\,\mathfrak{A}^{\delta\eta}}{\mu - m\,\nu\,\mathfrak{A}^{\delta\eta}}. \tag{4.42}$$

Here μ and ν are positive constants.
Step 3: Putting Eqs (4.4) and (4.5) into Eq (4.3) and collecting the coefficients equating to zero of each power of ζ yields the algebraic system of equations. To get unknown values, solve the system.
Step 4: Putting Eq (4.4) into Eq (4.3) yields the solutions to Eq (4.1).

4.1. Application

To determine $m = 1$ from Eq (3.7), Eq (4.4) becomes:

$$\mathfrak{Q}(\eta) = \mathfrak{w}_0 + \mathfrak{w}_1\zeta(\eta). \tag{4.43}$$

Putting Eq (4.43) with Eq (4.5) in Eq (3.7), we get this set of solutions after some computations with the help of software:
Set 1:

$$\mathfrak{w}_1 = \frac{\left(r_2 - \sqrt{r_2^2 - 4r_1r_3}\right)\mathfrak{w}_0}{2r_1}, \mathbb{P} = \frac{\frac{r_2}{\sqrt{r_2^2-4r_1r_3}} + 1}{d\mathfrak{w}_0}, v = -\frac{1}{\sqrt[6]{d^2\mathbb{Q}^2\left(r_2^2 - 4r_1r_3\right)\log^2(\mathfrak{A})}}.$$

Set 2:

$$\mathfrak{w}_1 \to \frac{\mathfrak{w}_0\left(r_2\sqrt{\left(r_2^2-4r_1r_3\right)}+\left(r_2^2-4r_1r_3\right)\right)}{2r_1\sqrt{\left(r_2^2-4r_1r_3\right)}}, \mathbb{P} \to \frac{1-\frac{r_2}{\sqrt{\left(r_2^2-4r_1r_3\right)}}}{d\mathfrak{w}_0}, v \to -\frac{\sqrt[3]{-1}}{\sqrt[6]{d^2\mathbb{Q}^2\left(r_2^2-4r_1r_3\right)\log^2(\mathfrak{N})}}.$$

Set 3:

$$\mathfrak{w}_1 \to \frac{\mathfrak{w}_0\left(r_2\sqrt{\left(r_2^2-4r_1r_3\right)}+\left(r_2^2-4r_1r_3\right)\right)}{2r_1\sqrt{\left(r_2^2-4r_1r_3\right)}}, \mathbb{P} \to \frac{1-\frac{r_2}{\sqrt{\left(r_2^2-4r_1r_3\right)}}}{d\mathfrak{w}_0}, v \to \frac{(-1)^{2/3}}{\sqrt[6]{d^2\mathbb{Q}^2\left(r_2^2-4r_1r_3\right)\log^2(\mathfrak{N})}}.$$

Here we take set 1 and generate different solutions as follows:
Case 1: when $\Omega = r_2^2 - 4r_1r_3 < 0$ and $r_3 \neq 0$:

$$\Psi(x,t) = \frac{\mathfrak{w}_0(r_2\left(\eta\sqrt{r_2^2-4r_1r_3}-2\log\left(\cos\left(\frac{\eta\sqrt{-\Omega}}{2}\right)\right)\right)+2\sqrt{r_2^2-4r_1r_3}\log\left(\cos\left(\frac{\eta\sqrt{-\Omega}}{2}\right)\right)-\eta r_2^2+4\eta r_1r_3)}{4r_1r_3}e^{\mu B(t)-\frac{1}{2}(\mu)^2t}, \tag{4.44}$$

$$\Psi(x,t) = \frac{\mathfrak{w}_0(r_2\left(\eta\sqrt{r_2^2-4r_1r_3}-2\log\left(\sin\left(\frac{\eta\sqrt{-\Omega}}{2}\right)\right)\right)+2\sqrt{r_2^2-4r_1r_3}\log\left(\sin\left(\frac{\eta\sqrt{-\Omega}}{2}\right)\right)-\eta r_2^2+4\eta r_1r_3)}{4r_1r_3}e^{\mu B(t)-\frac{1}{2}(\mu)^2t}, \tag{4.45}$$

$$\begin{aligned}\Psi(x,t) =& \frac{1}{4r_1r_3}(\mathfrak{w}_0(r_2\left(2\sqrt{\omega\nu}\tanh^{-1}\left(\tan\left(\frac{\eta\sqrt{-\Omega}}{2}\right)\right)-\log\left(\cos\left(\eta\sqrt{-\Omega}\right)\right)+\eta\sqrt{r_2^2-4r_1r_3}\right)\\ &+\sqrt{r_2^2-4r_1r_3}\left(\log\left(\cos\left(\eta\sqrt{-\Omega}\right)\right)-2\sqrt{\omega\nu}\tanh^{-1}\left(\tan\left(\frac{\eta\sqrt{-\Omega}}{2}\right)\right)\right)-\eta r_2^2+4\eta r_1r_3))e^{\mu B(t)-\frac{1}{2}(\mu)^2t},\end{aligned} \tag{4.46}$$

$$\begin{aligned}\Psi(x,t) =& \frac{1}{4r_1r_3}(\mathfrak{w}_0(r_2\left(-\sqrt{\omega\nu}\log\left(\tan\left(\frac{\eta\sqrt{-\Omega}}{2}\right)\right)-\log\left(\sin\left(\eta\sqrt{-\Omega}\right)\right)+\eta\sqrt{r_2^2-4r_1r_3}\right)\\ &+\sqrt{r_2^2-4r_1r_3}\left(\sqrt{\omega\nu}\log\left(\tan\left(\frac{\eta\sqrt{-\Omega}}{2}\right)\right)+\log\left(\sin\left(\eta\sqrt{-\Omega}\right)\right)\right)-\eta r_2^2+4\eta r_1r_3))e^{\mu B(t)-\frac{1}{2}(\mu)^2t},\end{aligned} \tag{4.47}$$

$$\begin{aligned}\Psi(x,t) =& \frac{1}{4r_1r_3}(\mathfrak{w}_0(r_2(-4\log(\sin(\frac{\eta\sqrt{-\Omega}}{4}))-4\log(\cos(\frac{\eta\sqrt{-\Omega}}{4}))+\eta\sqrt{r_2^2-4r_1r_3})\\ &+4(\sqrt{r_2^2-4r_1r_3}(\log(\sin(\frac{\eta\sqrt{-\Omega}}{4}))+\log(\cos(\frac{\eta\sqrt{-\Omega}}{4})))+\eta r_1r_3)-\eta r_2^2))e^{\mu B(t)-\frac{1}{2}(\mu)^2t},\end{aligned} \tag{4.48}$$

where $\eta = \nu x + \frac{c\Gamma(\beta+1)}{\alpha}t^\alpha$.
Case 2: when $\Omega = r_2^2 - 4r_1r_3 > 0$ and $r_3 \neq 0$:

$$\Psi(x,t) = \frac{\mathfrak{w}_0(r_2\left(\eta\sqrt{r_2^2-4r_1r_3}-2\log\left(\cosh\left(\frac{\eta\sqrt{\Omega}}{2}\right)\right)\right)+2\sqrt{r_2^2-4r_1r_3}\log\left(\cosh\left(\frac{\eta\sqrt{\Omega}}{2}\right)\right)-\eta r_2^2+4\eta r_1r_3)}{4r_1r_3}e^{\mu B(t)-\frac{1}{2}(\mu)^2t}, \tag{4.49}$$

$$\Psi(x,t) = \frac{\mathfrak{w}_0(r_2\left(\eta\sqrt{r_2^2-4r_1r_3}-2\log\left(\sinh\left(\frac{\eta\sqrt{\Omega}}{2}\right)\right)\right)+2\sqrt{r_2^2-4r_1r_3}\log\left(\sinh\left(\frac{\eta\sqrt{\Omega}}{2}\right)\right)-\eta r_2^2+4\eta r_1r_3)}{4r_1r_3}e^{\mu B(t)-\frac{1}{2}(\mu)^2t}, \tag{4.50}$$

$$\Psi(x,t) = \frac{1}{4r_1r_3}(\mathrm{w}_0(r_2(-2\sqrt{\omega\nu}\tan^{-1}(\tanh(\frac{\eta\sqrt{\Omega}}{2})) - \log(\cosh(\eta\sqrt{\Omega})) + \eta\sqrt{r_2^2-4r_1r_3}) + \sqrt{r_2^2-4r_1r_3}(2\sqrt{\omega\nu}\tan^{-1}(\tanh(\frac{\eta\sqrt{\Omega}}{2})) + \log(\cosh(\eta\sqrt{\Omega}))) - \eta r_2^2 + 4\eta r_1r_3))e^{\mu B(t)-\frac{1}{2}(\mu)^2t}, \tag{4.51}$$

$$\Psi(x,t) = \frac{1}{4r_1r_3}(\mathrm{w}_0(r_2(-(\sqrt{\omega\nu}+1)\log(\sinh(\frac{\eta\sqrt{\Omega}}{2})) + (\sqrt{\omega\nu}-1)\log(\cosh(\frac{\eta\sqrt{\Omega}}{2})) + \eta\sqrt{r_2^2-4r_1r_3}) + \sqrt{r_2^2-4r_1r_3}((\sqrt{\omega\nu}+1)\log(\sinh(\frac{\eta\sqrt{\Omega}}{2})) - (\sqrt{\omega\nu}-1)\log(\cosh(\frac{\eta\sqrt{\Omega}}{2}))) - \eta r_2^2 + 4\eta r_1r_3))e^{\mu B(t)-\frac{1}{2}(\mu)^2t}, \tag{4.52}$$

$$\Psi(x,t) = \frac{1}{4r_1r_3}(\mathrm{w}_0(r_2(4\log(\sinh(\frac{\eta\sqrt{\Omega}}{4})) - 4\log(\cosh(\frac{\eta\sqrt{\Omega}}{4})) + \eta\sqrt{r_2^2-4r_1r_3}) + 4(\sqrt{r_2^2-4r_1r_3}(\log(\cosh(\frac{\eta\sqrt{\Omega}}{4})) - \log(\sinh(\frac{\eta\sqrt{\Omega}}{4}))) + \eta r_1r_3) - \eta r_2^2))e^{\mu B(t)-\frac{1}{2}(\mu)^2t}, \tag{4.53}$$

where $\eta = \nu x + \frac{c\Gamma(\beta+1)}{\alpha}t^\alpha$.

Case 3: when $r_1r_3 > 0$ and $r_2 = 0$:

$$\Psi(x,t) = \mathrm{w}_0\left(\eta + \frac{\sqrt{-r_1^2r_3^2}\left(\frac{r_1}{r_3}\right)^{3/2}\log\left(\cos\left(\eta\sqrt{r_1r_3}\right)\right)}{r_1^3}\right)e^{\mu B(t)-\frac{1}{2}(\mu)^2t}, \tag{4.54}$$

$$\Psi(x,t) = \mathrm{w}_0\left(\eta + \frac{\sqrt{-r_1^2r_3^2}\left(\frac{r_1}{r_3}\right)^{3/2}\log\left(\sin\left(\eta\sqrt{r_1r_3}\right)\right)}{r_1^3}\right)e^{\mu B(t)-\frac{1}{2}(\mu)^2t}, \tag{4.55}$$

$$\Psi(x,t) = \frac{1}{2(r_1r_3)^{3/2}}(r_3\mathrm{w}_0(\sqrt{\frac{r_1}{r_3}}\sqrt{-r_1r_3}((\sqrt{\omega\nu}+1)\log(\sin(\eta\sqrt{r_1r_3}) + \cos(\eta\sqrt{r_1r_3})) - (\sqrt{\omega\nu}-1)\log(\cos(\eta\sqrt{r_1r_3}) - \sin(\eta\sqrt{r_1r_3}))) + 2\eta\sqrt{r_1r_3}r_1))e^{\mu B(t)-\frac{1}{2}(\mu)^2t}, \tag{4.56}$$

$$\Psi(x,t) = \frac{1}{4(r_1r_3)^{3/2}}(r_3\mathrm{w}_0(\sqrt{\frac{r_1}{r_3}}\sqrt{-r_1r_3}((\sqrt{\omega\nu}+1)\log(2\sin^2(\eta\sqrt{r_1r_3})) - (\sqrt{\omega\nu}-1)\log(\cos(2\eta\sqrt{r_1r_3})+1)) + 4\eta\sqrt{r_1r_3}r_1))e^{\mu B(t)-\frac{1}{2}(\mu)^2t}, \tag{4.57}$$

$$\Psi(x,t) = \mathrm{w}_0\left(\eta + \frac{\sqrt{-r_1^2r_3^2}\left(\frac{r_1}{r_3}\right)^{3/2}\log\left(\sin\left(\eta\sqrt{r_1r_3}\right)\right)}{r_1^3}\right)e^{\mu B(t)-\frac{1}{2}(\mu)^2t}, \tag{4.58}$$

where $\eta = \nu x + \frac{c\Gamma(\beta+1)}{\alpha}t^\alpha$.

Case 4: when $r_1r_3 < 0$ and $r_2 = 0$:

$$\Psi(x,t) = \mathrm{w}_0\left(\eta + \frac{\sqrt{-\frac{r_1}{r_3}}\log\left(\cosh\left(\eta\sqrt{-r_1r_3}\right)\right)}{r_1}\right)e^{\mu B(t)-\frac{1}{2}(\mu)^2t}, \tag{4.59}$$

$$\Psi(x,t) = \mathfrak{w}_0\left(\eta + \frac{\sqrt{-\frac{r_1}{r_3}}\log\left(\sinh\left(\eta\sqrt{-r_1r_3}\right)\right)}{r_1}\right)e^{\mu B(t)-\frac{1}{2}(\mu)^2t}, \tag{4.60}$$

$$\begin{aligned}\Psi(x,t) =& \frac{1}{2r_1r_3(\sqrt{\omega\nu} - i\sinh(2\eta\sqrt{-r_1r_3}) + i\sqrt{-\frac{r_1}{r_3}}\cosh(2\eta\sqrt{-r_1r_3}))}(\mathfrak{w}_0(r_3(2\eta\sqrt{\omega\nu}\sqrt{-\frac{r_1}{r_3}}\sqrt{-r_1r_3}\\
&- 2i\omega\nu\tan^{-1}(\tanh(\eta\sqrt{-r_1r_3})) - \sqrt{\omega\nu}\log(\cosh(2\eta\sqrt{-r_1r_3})) + 2\eta r_1(\sqrt{\omega\nu} - i\sinh(2\eta\sqrt{-r_1r_3})\\
&+ i\sqrt{-\frac{r_1}{r_3}}\cosh(2\eta\sqrt{-r_1r_3})) + 2\sqrt{\omega\nu}\sqrt{-\frac{r_1}{r_3}}\cosh(2\eta\sqrt{-r_1r_3})\tan^{-1}(\tanh(\eta\sqrt{-r_1r_3}))\\
&+ \sinh(2\eta\sqrt{-r_1r_3})(-2\sqrt{\omega\nu}\tan^{-1}(\tanh(\eta\sqrt{-r_1r_3})) - 2i\eta\sqrt{-\frac{r_1}{r_3}}\sqrt{-r_1r_3} + i\log(\cosh(2\eta\sqrt{-r_1r_3})))\\
&- i\sqrt{-\frac{r_1}{r_3}}\cosh(2\eta\sqrt{-r_1r_3})\log(\cosh(2\eta\sqrt{-r_1r_3}))) - 2i\eta r_1\sqrt{-r_1r_3}\cosh(2\eta\sqrt{-r_1r_3})))e^{\mu B(t)-\frac{1}{2}(\mu)^2t},\end{aligned} \tag{4.61}$$

$$\begin{aligned}\Psi(x,t) =& \frac{1}{2r_1}(\mathfrak{w}_0(\sqrt{\omega\nu}\log(\sinh(\eta\sqrt{-r_1r_3})) + (-(\sqrt{\omega\nu} - 1))\log(\cosh(\eta\sqrt{-r_1r_3}))\\
&+ 2\eta\sqrt{-\frac{r_1}{r_3}}\sqrt{-r_1r_3} + 2\eta r_1 + \log(\sinh(\eta\sqrt{-r_1r_3})))e^{\mu B(t)-\frac{1}{2}(\mu)^2t},\end{aligned} \tag{4.62}$$

$$\Psi(x,t) = \frac{\mathfrak{w}_0\left(\eta r_1 + \sqrt{-\frac{r_1}{r_3}}\left(\log\left(\sinh\left(\frac{1}{2}\eta\sqrt{-r_1r_3}\right)\right) + \log\left(\cosh\left(\frac{1}{2}\eta\sqrt{-r_1r_3}\right)\right)\right)\right)}{r_1}e^{\mu B(t)-\frac{1}{2}(\mu)^2t} \tag{4.63}$$

where $\eta = \nu x + \frac{c\Gamma(\beta+1)}{\alpha}t^\alpha$.
Case 5: when $r_3 = r_1$ and $r_2 = 0$:

$$\Psi(x,t) = \mathfrak{w}_0\left(\eta - \frac{\log(\cos(\eta r_1))}{\sqrt{-r_1^2}}\right)e^{\mu B(t)-\frac{1}{2}(\mu)^2t}, \tag{4.64}$$

$$\Psi(x,t) = \mathfrak{w}_0\left(\eta + \frac{\sqrt{-r_1^2}\log(\sin(\eta r_1))}{r_1^2}\right)e^{\mu B(t)-\frac{1}{2}(\mu)^2t}, \tag{4.65}$$

$$\Psi(x,t) = \mathfrak{w}_0\left(\eta + \frac{\left(-\sqrt{\omega\nu} - 1\right)\log(\cos(\eta r_1) - \sin(\eta r_1))}{2\sqrt{-r_1^2}} + \frac{\left(\sqrt{\omega\nu} - 1\right)\log(\sin(\eta r_1) + \cos(\eta r_1))}{2\sqrt{-r_1^2}}\right)e^{\mu B(t)-\frac{1}{2}(\mu)^2t}, \tag{4.66}$$

$$\Psi(x,t) = \frac{\mathfrak{w}_0\left(-\frac{\left(\sqrt{\omega\nu}-1\right)\sqrt{-r_1^2}\log(1-\cos(2\eta r_1))}{4r_1} - \frac{\left(-\sqrt{\omega\nu}-1\right)\sqrt{-r_1^2}\log(\cos(2\eta r_1)+1)}{4r_1} + \eta r_1\right)}{r_1}e^{\mu B(t)-\frac{1}{2}(\mu)^2t}, \tag{4.67}$$

$$\Psi(x,t) = \mathfrak{w}_0\left(\eta + \frac{\sqrt{-r_1^2}\log(\sin(\eta r_1))}{r_1^2}\right)e^{\mu B(t)-\frac{1}{2}(\mu)^2t}, \tag{4.68}$$

where $\eta = vx + \frac{c\Gamma(\beta+1)}{\alpha}t^{\alpha}$.
Case 6: when $r_3 = -r_1$ and $r_2 = 0$:

$$\Psi(x,t) = \mathfrak{w}_0\left(\eta + \frac{\log\left(\cosh\left(\eta r_1\right)\right)}{\sqrt{r_1^2}}\right)e^{\mu B(t)-\frac{1}{2}(\mu)^2 t}, \tag{4.69}$$

$$\Psi(x,t) = \mathfrak{w}_0\left(\eta + \frac{\log\left(\sinh\left(\eta r_1\right)\right)}{\sqrt{r_1^2}}\right)e^{\mu B(t)-\frac{1}{2}(\mu)^2 t}, \tag{4.70}$$

$$\Psi(x,t) = \frac{\mathfrak{w}_0\left(2\eta r_1^2 + \sqrt{r_1^2}\left(\log\left(\cosh\left(2\eta r_1\right)\right) - 2i\sqrt{\omega\nu}\tan^{-1}\left(\tanh\left(\eta r_1\right)\right)\right)\right)}{2r_1^2}e^{\mu B(t)-\frac{1}{2}(\mu)^2 t}, \tag{4.71}$$

$$\Psi(x,t) = \frac{\mathfrak{w}_0\left(\frac{\left(1-\sqrt{\omega\nu}\right)\sqrt{r_1^2}\log(\sinh(\eta r_1))}{2r_1} + \frac{\left(\sqrt{\omega\nu}+1\right)\sqrt{r_1^2}\log(\cosh(\eta r_1))}{2r_1} + \eta r_1\right)}{r_1}e^{\mu B(t)-\frac{1}{2}(\mu)^2 t}, \tag{4.72}$$

$$\Psi(x,t) = \frac{\mathfrak{w}_0\left(\eta r_1^2 + \sqrt{r_1^2}\left(\log\left(\sinh\left(\frac{\eta r_1}{2}\right)\right) + \log\left(\cosh\left(\frac{\eta r_1}{2}\right)\right)\right)\right)}{r_1^2}e^{\mu B(t)-\frac{1}{2}(\mu)^2 t}, \tag{4.73}$$

where $\eta = vx + \frac{c\Gamma(\beta+1)}{\alpha}t^{\alpha}$.
Case 7: when $r_2^2 - 4r_1r_3 = 0$:

$$\Psi(x,t) = -\frac{2\mathfrak{w}_0\log(\eta)}{r_2\log(\mathfrak{A})}e^{\mu B(t)-\frac{1}{2}(\mu)^2 t}, \tag{4.74}$$

where $\eta = vx + \frac{c\Gamma(\beta+1)}{\alpha}t^{\alpha}$.
Case 8: when $r_2 = \delta$, $r_1 = \delta m$ $(m \neq 0)$, and $r_3 = 0$:

$$\Psi(x,t) = \frac{1}{2}\mathfrak{w}_0\left(-\frac{\left(\delta - \sqrt{\delta^2}\right)\eta}{\delta} + 2\eta + \frac{\left(\delta - \sqrt{\delta^2}\right)\mathfrak{A}^{\delta\eta}}{\delta^2 m\log(\mathfrak{A})}\right)e^{\mu B(t)-\frac{1}{2}(\mu)^2 t}, \tag{4.75}$$

where $\eta = vx + \frac{c\Gamma(\beta+1)}{\alpha}t^{\alpha}$.

5. Interpretation of fractional and noise effects on the soliton solutions

In this section, the effect of noise and fractional order on the obtained soliton solutions shows kink and periodic behaviors through the following graphs by using the suitable values of the parameters of the solutions. Figure 1 shows 3D, 2D, and contour plots in (a) with $\mu = 0$ and in (b) with $\mu = 0.1$ at fixed values of $t = 0, 1, 2$ and a fractional order of $\alpha = 1$ usually to compare different parameter effects $\mu = 0, 0.1$, and in (c) and (d) with a fractional order of $\alpha = 0.5$ at fixed values of $t = 0, 1, 2$ usually to compare different parameter effects $\mu = 0, 0.1$ along other parameters $\sigma = 2$ with $r_1, r_2, r_3, \mathfrak{w}_0, v, c, \beta = 1, 2, 0.9, 2, -1, 1, 1$, $x \in$ [-2,2], $t \in$ [-1,1].

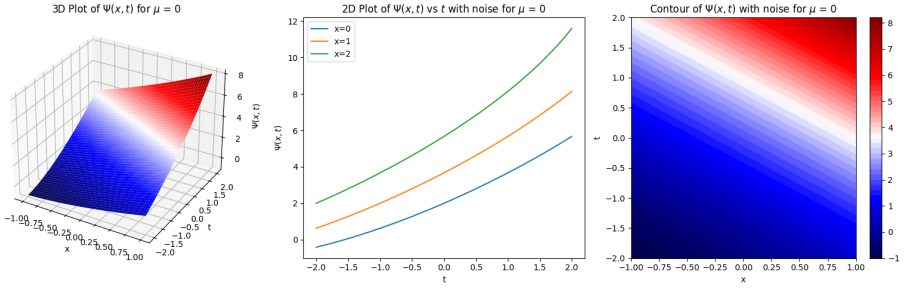

(a)

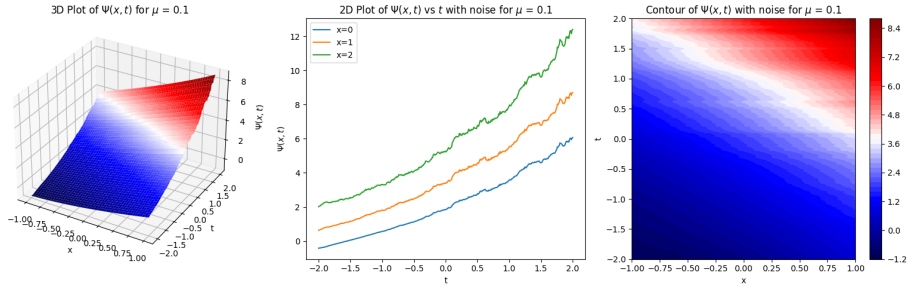

(b)

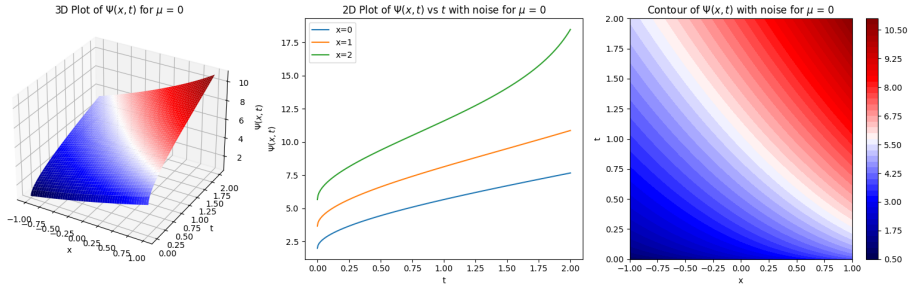

(c)

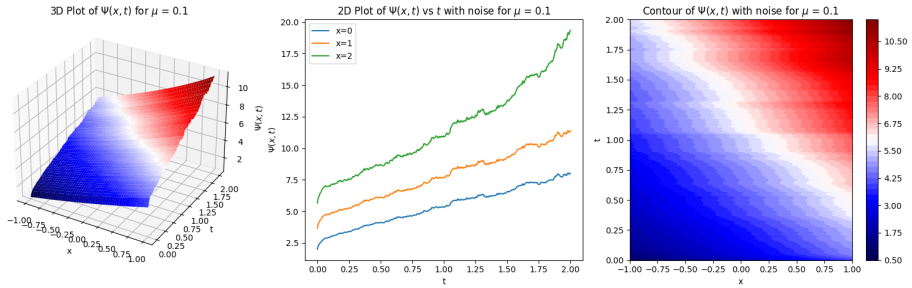

(d)

Figure 1. Kink behavior in 3D, 2D, and contour plots in (a) with $\mu = 0$, and in (b) with $\mu = 0.1$, and in (c) and (d) with a fractional order of $\alpha = 0.5$ for the solution to Eq (4.44).

Figure 2 shows 3D, 2D, and contour plots in (a) with $\mu = 0$ and in (b) with $\mu = 0.5$ at fixed values of $t = 0, 1, 2$ and a fractional order of $\alpha = 1$ usually to compare different parameter effects $\mu = 0, 0.5$, and in (c) and (d) with a fractional order of $\alpha = 0.5$ at fixed values of $t = 0, 1, 2$ usually to compare different

parameter effects $\mu = 0, 0.1$ along other parameters $\sigma = 2$ with $r_1, r_2, r_3, \varpi_0, v, c, \beta = 1, 4, 0.9, 2, 1, 1, 1$, $x \in$ [-5,5], $t \in$ [-1,1].

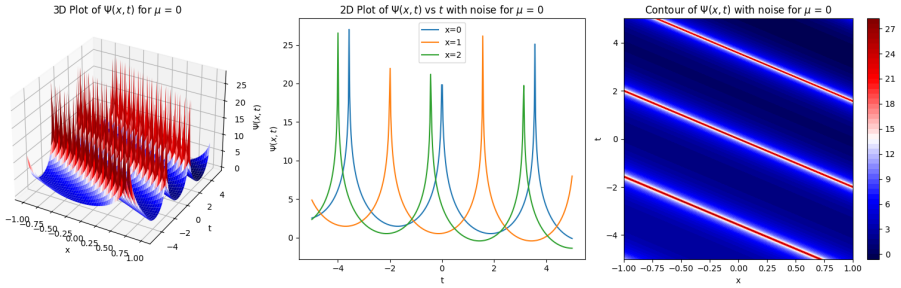

(a)

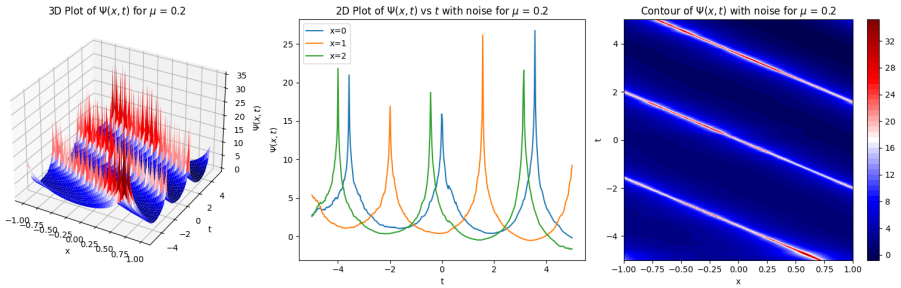

(b)

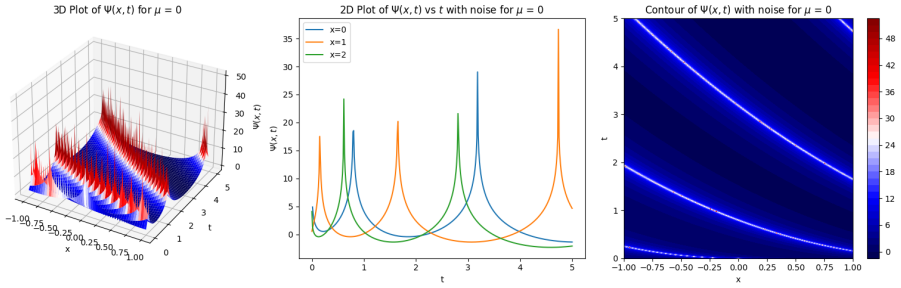

(c)

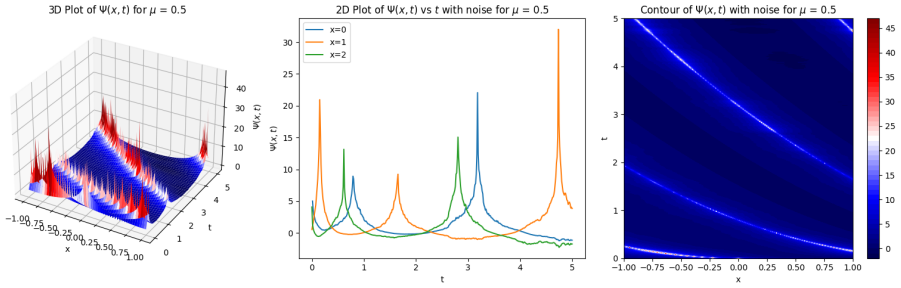

(d)

Figure 2. Periodic behavior in 3D, 2D, and contour plots in (a) with $\mu = 0$, and in (b) with $\mu = 0.5$, and in (c) and (d) with a fractional order of $\alpha = 0.5$ for the solution to Eq (4.45).

Figure 3 shows 3D, 2D, and contour plots in (a) with $\mu = 0$ and in (b) with $\mu = 0.1$ at fixed values of

$t = 0, 1, 2$ and a fractional order of $\alpha = 1$ usually to compare different parameter effects $\mu = 0, 0.1$, and in (c) and (d) with a fractional order of $\alpha = 0.5$ at fixed values of $t = 0, 1, 2$ usually to compare different parameter effects $\mu = 0, 0.1$ along other parameters $\sigma = 2$ with $r_1, r_2, r_3, \varpi_0, v, c, \beta = 1, 4, 0.9, 1, 1, 1, 1$, $x \in$ [-8,8], $t \in$ [-1,1].

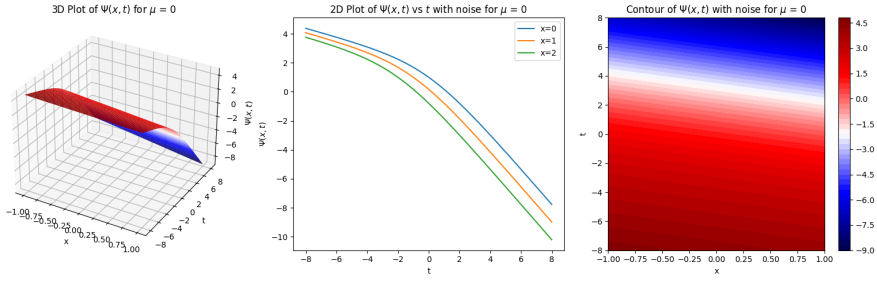

(a)

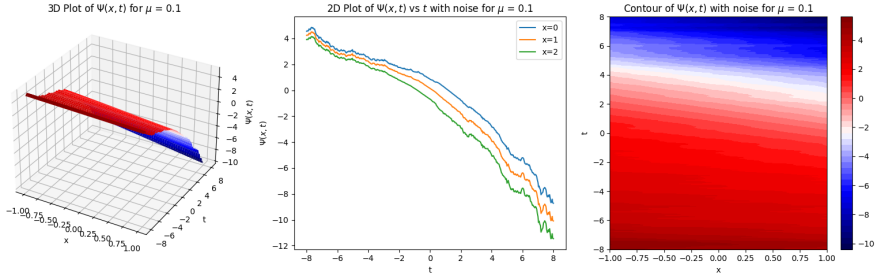

(b)

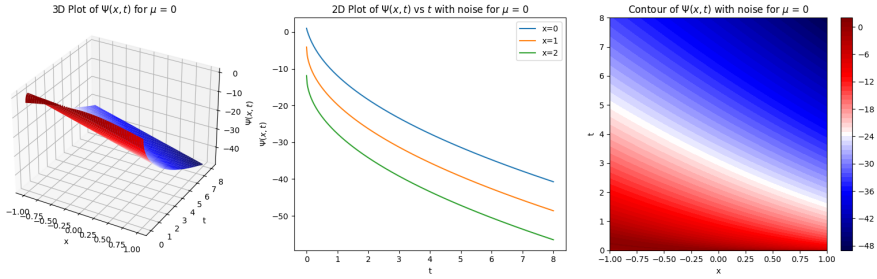

(c)

(d)

Figure 3. Kink behavior in 3D, 2D, and contour plots in (a) with $\mu = 0$, and in (b) with $\mu = 0.1$, and in (c) and (d) with a fractional order of $\alpha = 0.5$ for the solution to Eq (4.49).

6. Conclusions

In this work, we derived exact soliton solutions of the stochastic Poisson–Nernst–Planck system by incorporating Brownian motion and M-truncated fractional derivatives using the modified extended direct algebraic method. Our results reveal that stochastic noise and fractional-order effects significantly alter electro-diffusion behavior, giving rise to richer transport structures such as kink-type and periodic soliton patterns. These findings demonstrate the capability of the MEDAM to effectively handle nonlinear stochastic systems involving fractional operators. Moreover, the study broadens the analytical foundation for modeling stochastic electro-diffusion processes across biological, chemical, and physical settings. The method is limited to problems that admit compatible algebraic structures, and it may not efficiently capture highly irregular stochastic behaviors. Moreover, the method yields exact solutions only for specific parameter regimes, which restricts its applicability to more complex or strongly nonlinear stochastic systems. In the end, we graphically demonstrated the effect of noise and the fractional order of derivation in 3D, 2D, and contour surfaces.

Author contributions

Waseem Razzaq and Asim Zafar: Idea, methodology, investigation, writing – review and editing; Abdulaziz Khalid Alsharidi and Mohammed Ahmed Alomair: Formal analysis, resources, visualization, writing – review and editing. All authors have read and approved the final version of the manuscript for publication.

Use of Generative-AI tools declaration

The authors declare they have not used Artificial Intelligence (AI) tools in the creation of this article.

Funding

This work was supported by the Deanship of Scientific Research, Vice Presidency for Graduate Studies and Scientific Research, King Faisal University, Saudi Arabia [Grant No. KFU254478].

Conflict of interest

The authors declare there is no conflict of interest.

References

1. M. A. Elfouly, M. A. Sohaly, M. E. Fares, FitzHugh–Nagumo model in neutral delay differential equation representation, *Res. Sq.*, 2024, Preprint. https://doi.org/10.21203/rs.3.rs-5048513/v1
2. A. De Laire, Recent results for the Landau–Lifshitz equation, *SeMA*, **79** (2022), 253–295. https://doi.org/10.1007/s40324-021-00254-1

3. A. N. Landge, B. M. Jordan, X. Diego, P. Müller, Pattern formation mechanisms of self-organizing reaction–diffusion systems, *Dev. Biol.*, **460** (2020), 2–11. https://doi.org/10.1016/j.ydbio.2019.10.031

4. S. Khuri, New approach for soliton solutions for the (2+1)-dimensional KdV equation describing shallow water wave, *Int. J. Numer. Methods Heat Fluid Flow*, **33** (2023), 965–973. https://doi.org/10.1108/HFF-08-2022-0498

5. A. Bocharov, O. Y. Tsvelodub, Nonlinear steady-state traveling solutions of the Kuramoto–Sivashinsky equation coupled with the linear dissipative equation, *Chaos Soliton Fract.*, **198** (2025), 116572. https://doi.org/10.1016/j.chaos.2025.116572

6. G. Q. Xu, A. M. Wazwaz, A new (n+1)-dimensional generalized Kadomtsev–Petviashvili equation: Integrability characteristics and localized solutions, *Nonlinear Dyn.*, **111** (2023), 9495–9507. https://doi.org/10.1007/s11071-023-08343-8

7. H. H. Hussein, H. M. Ahmed, S. A. Kandil, W. Alexan, Unveiling diverse solitons in the quintic perturbed Gerdjikov–Ivanov model via a modified extended mapping method, *Sci. Rep.*, **15** (2025), 15881. https://doi.org/10.1038/s41598-025-97981-6

8. U. Akpan, L. Akinyemi, D. Ntiamoah, A. Houwe, S. Abbagari, Generalized stochastic Korteweg–de Vries equations, their Painlevé integrability, N-soliton and other solutions, *Int. J. Geom. Methods Mod. Phys.*, **21** (2024), 2450128. https://doi.org/10.1142/S0219887824501287

9. T. Nan, M. Z. Baber, N. Ahmed, M. S. Iqbal, U. Demirbilek, H. Rezazadeh, Effects of Brownian motion on solitary wave structures for 1D stochastic Poisson–Nernst–Planck system in electrobiochemical media, *Int. J. Geom. Methods Mod. Phys.*, **21** (2024), 2450225. https://doi.org/10.1142/S0219887824502256

10. W. Razzaq, A. Zafar, Machine learning-enhanced soliton solutions for the Lonngren-wave equation: An integration of Painlevé analysis and Hirota bilinear method, *Rend. Lincei Sci. Fis. Nat.*, **36** (2025), 917–932. https://doi.org/10.1007/s12210-025-01354-0

11. S. Kumar, S. K. Dhiman, Exploring cone-shaped solitons, breather and lump-form solutions using the Lie symmetry method and unified approach to a coupled breaking soliton model, *Phys. Scr.*, **99** (2024), 025243. https://doi.org/10.1088/1402-4896/ad1d9e

12. N. A. Kudryashov, A. Biswas, Q. Zhou, Y. Yildirim, Painlevé analysis and chiral solitons from quantum Hall effect, *Contemp. Math.*, **542** (2024), 4384–4398. https://doi.org/10.37256/cm.5420245313

13. S. Naowarat, S. Saifullah, S. Ahmad, M. De la Sen, Periodic, singular and dark solitons of a generalized geophysical KdV equation by using the tanh–coth method, *Symmetry*, **15** (2023), 135. https://doi.org/10.3390/sym15010135

14. S. Behera, Multiple soliton solutions of some conformable fractional nonlinear models using the sine–cosine method, *Opt. Quant. Electron.*, **56** (2024), 1235. https://doi.org/10.1007/s11082-024-06403-w

15. W. Razzaq, A. Zafar, A. K. Alsharidi, M. A. Alomair, New three-wave and periodic solutions for the nonlinear (2+1)-dimensional Burgers equations, *Symmetry*, **15** (2023), 1573. https://doi.org/10.3390/sym15081573

16. A. K. S. Hossain, M. K. Islam, H. Akter, M. A. Akbar, Exact and soliton solutions of nonlinear evolution equations in mathematical physics using the generalized G'/G-expansion approach, *Phys. Scr.*, **100** (2024), 015269. https://doi.org/10.1088/1402-4896/ad9da1

17. I. Samir, H. M. Ahmed, W. Rabie, W. Abbas, O. Mostafa, Construction of optical solitons of generalized nonlinear Schrödinger equation with quintuple power-law nonlinearity using Exp-function, projective Riccati and new generalized methods, *AIMS Mathematics*, **10** (2025), 3392–3407. https://doi.org/10.3934/math.2025157

18. A. Zafar, W. Razzaq, H. Rezazadeh, M. Eslami, The complex hyperbolic Schrödinger dynamical equation with a truncated M-fractional derivative via simplest equation method, *Comput. Methods Differ. Equ.*, **12** (2024), 44–55. https://doi.org/10.22034/cmde.2022.40084.1747

19. M. I. Khan, J. Sabi'u, A. Khan, S. Rehman, A. Farooq, Unveiling new insights into soliton solutions and sensitivity analysis of the Shynaray-IIA equation through an improved generalized Riccati equation mapping method, *Opt. Quant. Electron.*, **56** (2024), 1339. https://doi.org/10.1007/s11082-024-07271-0

20. N. Sun, Y. Wang, Exact solutions of the generalized third-order nonlinear Schrödinger equation using the trial equation method and complete discriminant system for polynomial method with applications in optical fibers, *Int. J. Appl. Comput. Math.*, **11** (2025), 65. https://doi.org/10.1007/s40819-025-01872-3

21. Z. Z. Si, Z. T. Ju, L. F. Ren, X. P. Wang, B. A. Malomed, C. Q. Dai, Polarization-induced buildup and switching mechanisms for soliton molecules composed of noise-like-pulse transition states, *Laser Photon. Rev.*, **19** (2025), 2401019. https://doi.org/10.1002/lpor.202401019

22. D. S. Mou, Z. Z. Si, W. X. Qiu, C. Q. Dai, Optical soliton formation and dynamic characteristics in photonic moiré lattices, *Opt. Laser Technol.*, **181** (2025), 111774. https://doi.org/10.1016/j.optlastec.2024.111774

23. M. Waqar, K. M. Saad, M. Abbas, M. Vivas-Cortez, W. M. Hamanah, Diverse wave solutions for the (2+1)-dimensional Zoomeron equation using the modified extended direct algebraic approach, *AIMS Mathematics*, **10** (2025), 12868–12887. https://doi.org/10.3934/math.2025578

24. F. Ashraf, R. Ashraf, A. Akgül, Traveling wave solutions of the Hirota–Ramani equation by modified extended direct algebraic and new extended direct algebraic method, *Int. J. Mod. Phys. B*, **38** (2024), 2450329. https://doi.org/10.1142/S0217979224503296

25. H. Qawaqneh, Y. Alrashedi, H. Ahmad, A. Bekir, Discovery of exact solitons to the fractional KP-MEW equation with stability analysis, *Eur. Phys. J. Plus*, **140** (2025), 316. https://doi.org/10.1140/epjp/s13360-025-06188-1

26. A. Amer, S. M. Boulaaras, A. Althobaiti, S. Althobaiti, H. U. Rehman, Soliton dynamics and numerical insights for the Shynaray-IIA equation, *Int. J. Mod. Phys. B*, **39** (2025), 2550203. https://doi.org/10.1142/S0217979225502030

27. T. Shahzad, M. O. Ahmed, M. Z. Baber, N. Ahmed, A. Akgül, T. Abdeljawad, et al., Explicit solitary wave structures for the fractional-order Sobolev-type equations and their stability analysis, *Alex. Eng. J.*, **92** (2024), 24–38. https://doi.org/10.1016/j.aej.2024.02.032

28. M. S. Iqbal, M. Inc, Optical soliton solutions for stochastic Davey–Stewartson equation under the effect of noise, *Opt. Quant. Electron.*, **56** (2024), 1148. https://doi.org/10.1007/s11082-024-06453-0

Appendix

To justify the identity $\mathbb{E}\left[e^{\mu B(t)}\right] = e^{\frac{1}{2}\mu^2 t}$ used in Eq (3.3), we note that for a standard Brownian motion $B(t)$, the marginal distribution at each fixed time t is Gaussian with mean 0 and variance t, i.e., $B(t) \sim \mathcal{N}(0, t)$. The moment generating function of a normal random variable $X \sim \mathcal{N}(m, \sigma^2)$ is given by

$$\mathbb{E}[e^{sX}] = \exp\left(sm + \tfrac{1}{2}s^2\sigma^2\right).$$

By taking $m = 0$, $\sigma^2 = t$, and $s = \mu$, we immediately obtain

$$\mathbb{E}\left[e^{\mu B(t)}\right] = \exp\left(\tfrac{1}{2}\mu^2 t\right),$$

which is the formula used in our derivation. For completeness, we have included the explicit integral derivation based on completing the square:

$$\mathbb{E}\left[e^{\mu B(t)}\right] = \frac{1}{\sqrt{2\pi t}} \int_{-\infty}^{\infty} e^{\mu x}\, e^{-x^2/(2t)}\, dx = \frac{1}{\sqrt{2\pi t}} \int_{-\infty}^{\infty} \exp\left(-\frac{1}{2t}(x^2 - 2\mu t x)\right) dx.$$

Completing the square,

$$x^2 - 2\mu t x = (x - \mu t)^2 - \mu^2 t^2,$$

so

$$\mathbb{E}\left[e^{\mu B(t)}\right] = e^{\frac{1}{2}\mu^2 t} \cdot \frac{1}{\sqrt{2\pi t}} \int_{-\infty}^{\infty} e^{-(x-\mu t)^2/(2t)}\, dx.$$

The remaining integral equals 1 because it is the density of a normal distribution with variance t. Therefore,

$$\mathbb{E}\left[e^{\mu B(t)}\right] = e^{\frac{1}{2}\mu^2 t}.$$